

# Syngas Formation by Nickel and Iron Catalysts for Partial Oxidation of Methane with Microwave Assistance

Chin Chung Lo,<sup>1</sup> Chien Li Lee,<sup>2</sup> and Chih-Ju G. Jou<sup>1\*</sup>

<sup>1</sup>Department of Safety, Health and Environmental Engineering,  
National Kaohsiung University of Science and Technology, 2 Juoyue Rd, Nantz District, Kaohsiung 811, Taiwan

<sup>2</sup>Research and Development Center for Water Resource and Conservation,  
National Kaohsiung University of Science and Technology, 2 Juoyue Rd, Nantz District, Kaohsiung 811, Taiwan

(Received August 2, 2019; accepted December 6, 2019)

**Keywords:** microwave, syngas, microscale Ni and Fe catalysts

In this study, microscale nickel (Ni, 0.33 wt%) and iron (Fe, 0.26 wt%) catalysts coated on cordierite particles were used in the partial oxidation of methane to form syngas by a microwave-assisted process. Microwave treatment can be applied by coupling with materials having higher dielectric loss values. This is because Ni has more electron holes and a higher activity than Fe, and Ni-based catalysts produce heat much faster than Fe-based catalysts upon microwave treatment (208.8 vs 26 °C/min). Under the same experimental conditions of a volumetric ratio of CH<sub>4</sub>/air of 1:1, a microwave output power of 450 W, and the reaction time set to 360 min, higher H<sub>2</sub> and CO yields were obtained with the Ni catalyst than with the Fe catalyst (54.7 vs 46.0% for H<sub>2</sub> and 19.7 vs 14.4% for CO). The coke content was determined to be 0.4 wt% for the Ni catalyst and 0.51 wt% for the Fe catalyst. The shape of the coke was different for the two catalysts; finely shaped coke was observed for the Ni catalyst, whereas thicker multilayered coke appeared on the Fe catalyst.

## 1. Introduction

Syngas is mainly composed of CO and H<sub>2</sub>, and is an important raw material widely used to produce ammonia and methanol in the chemical and petrochemical industries and to generate gas-liquid fuels in the metal industry and metal technologies.<sup>(1–3)</sup>

The primary raw material for producing syngas is methane (CH<sub>4</sub>) or natural gas because the cost of producing the final product is relatively low.<sup>(2)</sup> Three methods are generally used to produce syngas from methane: steam reforming, dry rearrangement, and catalytic partial oxidation.<sup>(4–6)</sup> The partial oxidation of CH<sub>4</sub> has gradually become a promising alternative to replace the steam reforming method<sup>(7,8)</sup> owing to three key advantages. First, partial oxidation is a mild exothermic reaction. Secondly, the 2:1 (v/v) ratio of H<sub>2</sub>/CO produced from the partial reaction is an ideal ratio for downstream processes, such as the synthesis of methanol, and the Fischer–Tropsch reaction.<sup>(9)</sup> Lastly, the catalyst residence time in partial oxidation is only of millisecond order, which is much shorter than that in the steam reforming method (~0.5–1 s). The water-gas shift is also another important reaction in partial oxidation, which assists

\*Corresponding author: e-mail: george@nkust.edu.tw  
<https://doi.org/10.18494/SAM.2020.2580>

hydrogen production with a higher  $H_2/CO$  molar ratio.<sup>(10,11)</sup> Therefore, the partial oxidation method could achieve the same or greater production of syngas with less investment and a smaller production scale, giving it better development prospects for the future.<sup>(12,13)</sup>

Nobel metal catalysts have been widely used in the partial oxidation reaction because of their high activity, selectivity, and stability under various reaction conditions. The order of catalytic activity is  $Ph\sim Ru > Ir > Pt > Pd$  under the same conditions. Figen and Baykara showed that Ni has a high catalytic activity in the steam reforming reaction,<sup>(14)</sup> where the methane conversion rate is more than 97%. For the partial oxidation method, Corbo and Migliardini showed that a Ni catalyst has a higher  $H_2$  selectivity than a Pt– $CeO_2$  catalyst, along with a higher  $H_2$  yield and a higher carbon accumulation rate. However, the amount of carbon deposited is significantly higher with a Ni catalyst than with a Pt– $CeO_2$  catalyst.<sup>(15)</sup>

In the treatment of materials with microwave energy, the microwave energy is transferred directly to the materials through the molecular interaction with the electromagnetic field. Conventionally, thermal energy is transferred to materials through the convection, conduction, and radiation of heat from the surfaces of the materials.<sup>(16,17)</sup> Microwave heating is delivered directly to the interior of materials. Its advantages include homogeneous and rapid heating, reduced energy consumption and chemical reaction time, selective heating, and non-contact heating.<sup>(18–21)</sup> Microwave heat treatment technology has been applied to a variety of fields, such as sintering and ceramic preheating,<sup>(21)</sup> food processing, and the destruction of bacteria.<sup>(16)</sup> Promising results have been obtained for the treatment of halogen pollutants by microwave treatment together with catalyst media (zero-valent Cu or Fe nanoparticles and  $TiO_2$ ).<sup>(22–24)</sup>

In this study, Ni and Fe catalysts are used for the partial oxidation of  $CH_4$  with microwave assistance, since both Ni and Fe catalysts have high dielectric constants, enabling them to absorb microwave energy and convert it to the heat energy required for the partial oxidation to obtain syngas.

## 2. Equipment and Methods

### 2.1 Preparation of catalysts

To prepare microscale Ni/cordierite and microscale Fe/cordierite, 20 g of cordierite particles were washed in boiling HCl (37% or 1 M) solution for 30 min to increase their surface area. The acid-washed cordierite particles were suspended in deionized (DI) water while subject to ultrasonic agitation for 30 min, then boiled for 30 min to remove the free acid. These cleaning/washing procedures were repeated several times until the cordierite became neutral. After drying in a 105 °C oven for 24 h, the treated cordierite particles were suspended in  $Ni(NO_3)_2$  or  $FeCl_3$  solution (3 wt%  $Ni(NO_3)_2 \cdot 6H_2O$  or 3 wt%  $FeCl_3 \cdot H_2O$  in DI water), then the suspension was agitated at 200 rpm in a 25 °C water bath for 4 h. The particles were then removed from the treated solutions, then 0.75 M  $NaBH_4$  solution was added dropwise until all the cordierite particles were submerged in  $NaBH_4$  solution. The unabsorbed  $Ni(NO_3)_2$  and  $FeCl_3$  were removed from the cordierite particles by washing with DI water.

## 2.2 Experimental method

A microwave oven with a frequency of 2.45 GHz and a maximum output power of 750 W was equipped with a proportional–integral–derivative (PID) controller to control the output power to 450 W. Fourteen grams of microscale Ni/cordierite or microscale Fe/cordierite catalyst prepared as described above was placed in an 80 mL quartz glass reactor with 40 small holes evenly distributed at the bottom. The reactor was placed at the center of the microwave oven, as shown in Fig. 1. The experimental conditions were as follows. 1) Continuous microwave irradiation was performed for 6 h. 2) A CH<sub>4</sub>/air mixture passed through the holes at the bottom of the reactor with an influent volumetric flow rate of either 10/10 (mL/min) (CH<sub>4</sub>/air ratio of 1:1) or 10/20 (mL/min) (CH<sub>4</sub>/air ratio of 1:2).

## 2.3 Analyses

The chemical composition of the organic intermediates and final products was analyzed using a gas chromatography–thermal conductivity detector (GC–TCD, SHIMADZU, GC-2014). The composition of the tail gas was analyzed by gas chromatography (GC), with 1  $\mu$ l samples taken every 30 min with three replicates. The material balance was calculated from the oxygen component, utilizing the composition analysis results obtained from GC.

The carrying gas (Ar) flow rate was maintained at 25 mL/min. The GC oven temperature was programmed to increase from 40 to 210 °C at a ramp rate of 40 °C/min, then the temperature was held for 5 min at 210 °C. The GC injector temperature was set at 120 °C. A type K thermocouple with a full-scale error of 0.3% was used for temperature measurement. A carbon determinator (Eltra, CS 800) was used to analyze the coke content of the catalyst. Images produced by scanning electron microscopy (SEM) (Hitachi, SU8000) were used to observe the changes in the surface structure. An accelerated surface area and porosimetry system (Micromeritics, ASAP 2020) was used to measure the changes in the surface of the catalyst.

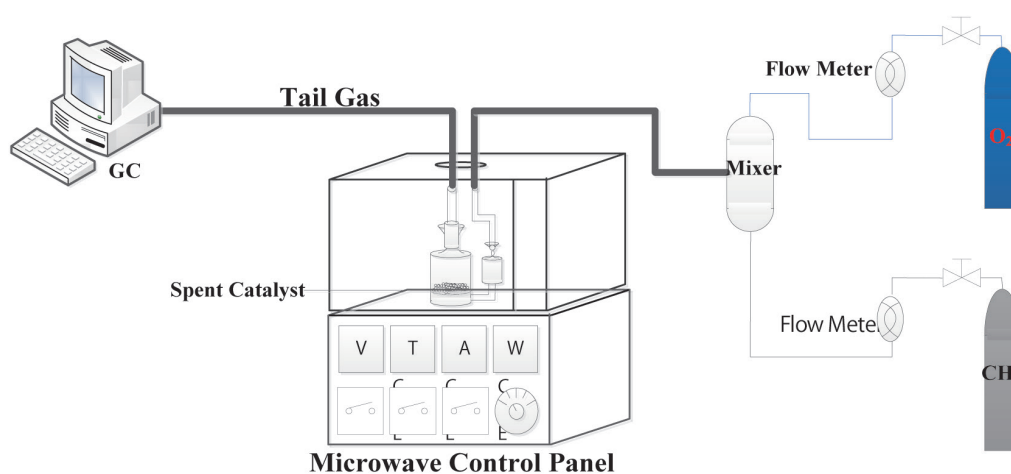


Fig. 1. (Color online) Diagram of the experimental setup.

### 3. Results and Discussion

#### 3.1 Preparation of Ni/cordierite and Fe/cordierite catalysts

After the cordierite particles were acidified and washed, they were dried then calcined at 550 °C to complete the pretreatment of the catalyst carrier. As a result of the pretreatment, the mean specific surface area of the carrier increased by 21% (from 0.43 to 0.52 m<sup>2</sup>/g).

After the pretreatment, the carrier was immersed in the Ni(NO<sub>3</sub>)<sub>2</sub> or FeCl<sub>3</sub> solution for 6 h, as a result of which the amounts of microscale Ni and Fe coated onto the carriers were 0.33 and 0.26 wt%, respectively. The results of energy-dispersive X-ray spectroscopy (EDS) analysis for the cordierite carrier, Ni/cordierite, and Fe/cordierite are shown in Figs. 2(a)–2(c), respectively, and the corresponding SEM images of their surfaces are shown in Fig. 3. The surface of the cordierite carrier after the pretreatment was smooth and free of particles [Fig. 3(a)], whereas irregular particles accumulated on the surface after the carrier was coated with the Ni catalyst [Fig. 3(b)]. Small flakes were observed on the surface of the smaller particles after the carrier was coated with the Fe catalyst [Fig. 3(c)].

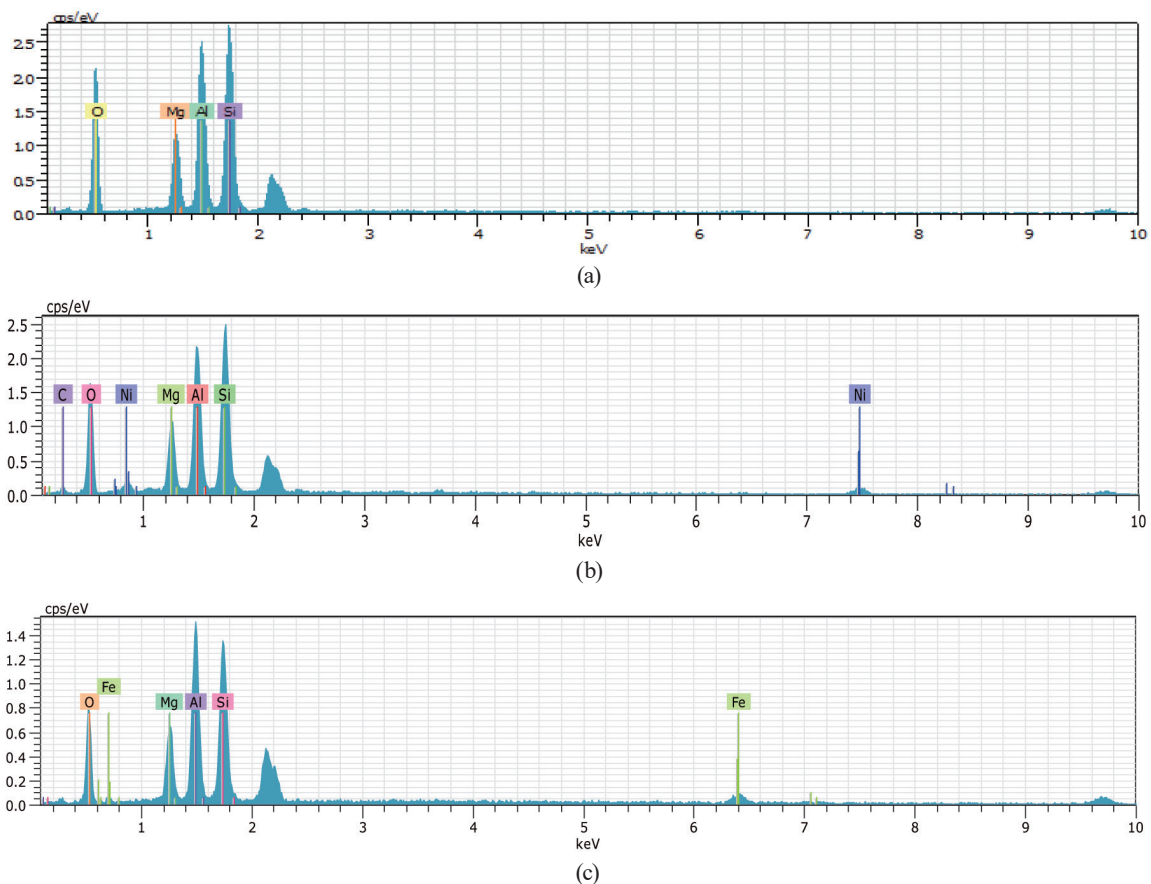


Fig. 2. (Color online) EDS spectra: (a) cordierite, (b) Ni/cordierite, and (c) Fe/cordierite.

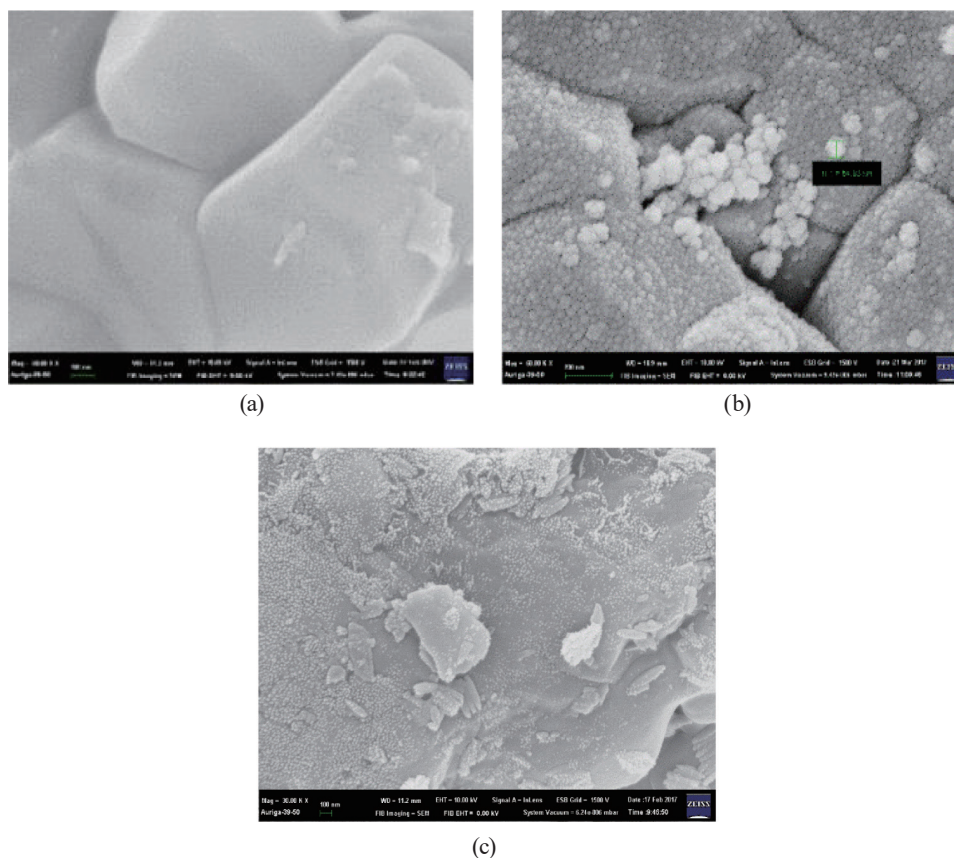


Fig. 3. (Color online) SEM images: (a) cordierite, (b) Ni/cordierite, and (c) Fe/cordierite.

### 3.2 Effect of Ni/cordierite and Fe/cordierite catalysts on syngas yield

The first step of the catalytic partial oxidation of  $\text{CH}_4$  is deep oxidation, which is an exothermic reaction involving the combustion of  $\text{CH}_4$  with oxygen to form  $\text{CO}_2$  and  $\text{H}_2\text{O}$ . The second step is the recombination of the residual methane with  $\text{H}_2\text{O}$  and  $\text{CO}_2$  to form  $\text{H}_2$  and  $\text{CO}$ , which is an endothermic reaction.<sup>(4)</sup>

The  $\text{H}_2$  and  $\text{CO}$  yields obtained when the reaction was carried out with the Ni/cordierite catalyst in a microwave oven for 360 min under 450 W power are shown in Figs. 4 and 5, respectively. When the  $\text{CH}_4/\text{air}$  influent volumetric ratio was 1:1  $\text{CH}_4/\text{air}$  (10/10 mL/min), the  $\text{H}_2$  and  $\text{CO}$  yields were 54.7 and 19.7%, respectively. A lower ratio of  $\text{CH}_4$  was expected to reduce the rate of recombination reaction with  $\text{H}_2\text{O}$  and  $\text{CO}_2$ , resulting in lower  $\text{H}_2$  and  $\text{CO}$  yields. When  $\text{CH}_4/\text{air}$  influent volumetric ratio was 1:2 (10/20 mL/min), the  $\text{H}_2$  and  $\text{CO}$  yields were reduced to 42.2 and 13.8%, respectively.

In addition, under the same experimental conditions [an influent volume ratio of 1:1  $\text{CH}_4/\text{air}$  (10/10 mL/min), a microwave energy of 450 W, and an exposure time of 360 min], the Ni/cordierite catalyst had higher yields than the Fe/cordierite catalyst. The  $\text{H}_2$  yield was 54.7% for Ni/cordierite, compared with 46.0% for Fe/cordierite (Fig. 6), and the  $\text{CO}$  yield was 19.7% for Ni/cordierite, compared with 14.4% for Fe/cordierite (Fig. 7). Compared with Fe, Ni

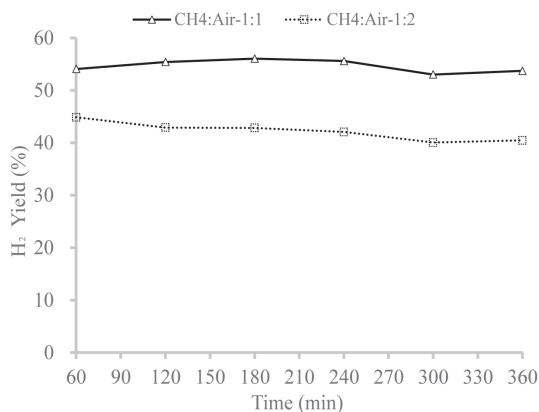


Fig. 4. Yield of H<sub>2</sub> for different CH<sub>4</sub>/air ratios with Ni/cordierite catalyst.

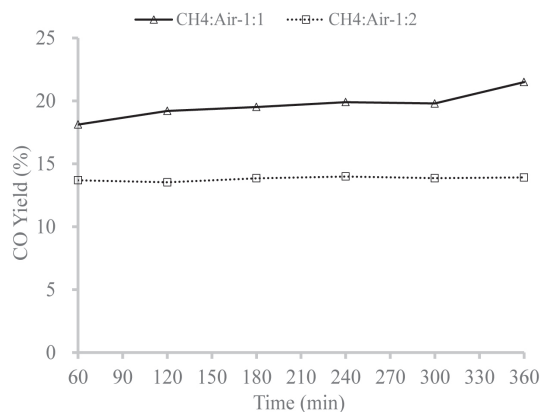


Fig. 5. Yield of CO for different CH<sub>4</sub>/air ratios with Ni/cordierite catalyst.

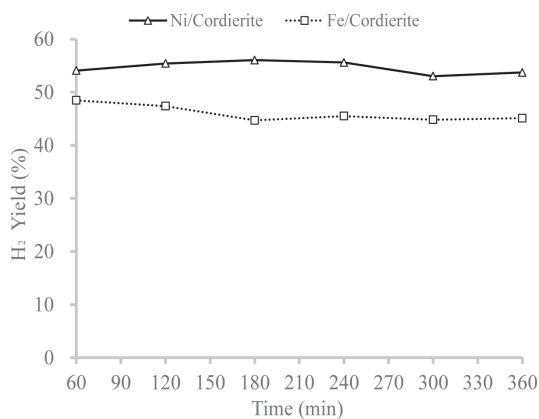


Fig. 6. Yield of H<sub>2</sub> for Ni/cordierite and Fe/cordierite catalysts.

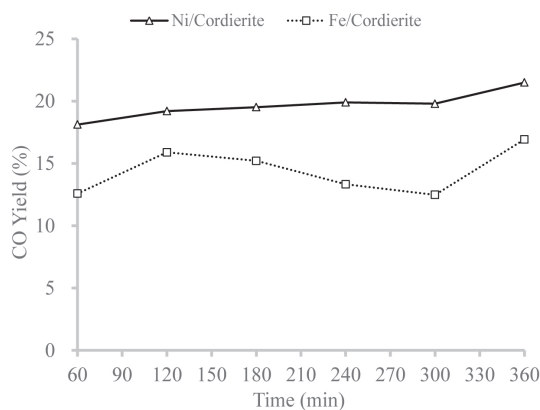


Fig. 7. Yield of CO for Ni/cordierite and Fe/cordierite catalysts.

has more electron holes, making it more active. It also had a much higher heating rate under microwave treatment of 208.8 °C/min, compared with 26 °C/min for the Fe/cordierite catalyst.

### 3.3 Structure analysis of catalysts

Under a CH<sub>4</sub>/air intake ratio of 1:1, an exposure time of 360 min, and a microwave energy of 450 W, the Ni/cordierite catalyst had a higher activity, enabling the easy deposition of coke. The initial coke content was determined to be zero before the reaction and 0.44 wt% after the reaction for Ni/cordierite at a CH<sub>4</sub>/air intake ratio of 1:1. The SEM image of Ni/cordierite in Fig. 8(a) shows filamentous coke deposits on the Ni/cordierite surface, consistent with the study of Suelves *et al.*<sup>(25)</sup>

Because the heating rate of Fe/cordierite was much lower than that of Ni/cordierite, the average bed temperature was lower for the Fe/cordierite catalyst (355 °C) than for the Ni/cordierite catalyst under the same conditions. The coke content on Fe/cordierite (1.04 wt%)

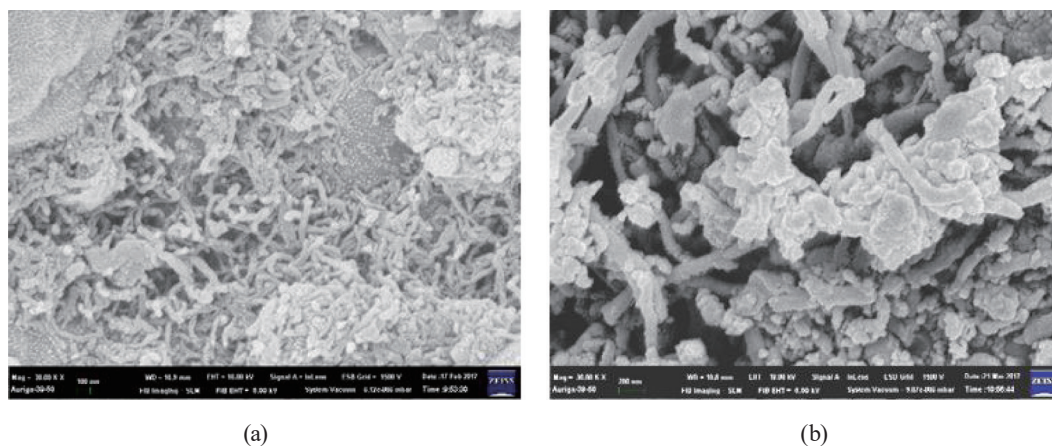


Fig. 8. (Color online) SEM images after microwave treatment: (a) Ni/cordierite and (b) Fe/cordierite.

was higher than that on Ni/cordierite (0.44 wt%) after the microwave treatment with the  $\text{CH}_4/\text{air}$  influent ratio maintained at 1:1. The SEM image in Fig. 8(b) also shows that the coke deposited on the Fe/cordierite surface was filamentous but thicker than that on the Ni/cordierite surface. In addition, some spherical coke particles were deposited on Fe/cordierite but not on Ni/cordierite.

#### 4. Conclusion

In this study, the microwave energy absorbed by cordierite particles coated with microscale Ni or Fe as a catalyst was converted to heat energy provided for syngas production. We obtained  $\text{H}_2$  and CO yields of 54.7 and 19.7% with the Ni/cordierite catalyst upon the partial oxidation of  $\text{CH}_4$ , compared with the 46.0 and 14.4%  $\text{H}_2$  and CO yields with the Fe/cordierite catalyst under the same conditions ( $\text{CH}_4/\text{air}$  volume ratio 1:1, microwave power 450 W, and reaction time 360 min), respectively. This might have been due to the electronic configuration of Ni, which has more electron holes and is more active than Fe. The heating rate was much higher with Ni/cordierite than with Fe/cordierite (208.8 vs 26  $^\circ\text{C min}^{-1}$ ). The average reaction temperature was also higher with Ni/cordierite than with Fe/cordierite (580 vs 355  $^\circ\text{C}$ ). Moreover, the amount of coke deposited on the surface of the catalyst was determined to be 0.44 wt% for Ni/cordierite and 1.04 wt% for Fe/cordierite. In addition, although the coke was filamentous for both catalysts, it was found that the layer of carbon deposited on the surface of Ni/cordierite was thinner than that deposited on the surface of Fe/cordierite. It was also observed that some spherical coke particles were deposited only on the surface of the Fe/cordierite catalyst.

By studying physical characteristics, such as the dielectric loss and electron hole density, on various metal catalysts for different experimental conditions, one can find the optimal conditions for economically producing syngas through a tail gas. This is an innovative concept for industrial application.

## References

- 1 A. Donazzi, D. Livio, C. Diehm, A. Beretta, G. Groppi, and P. Forzatti: *Appl. Catal. A* **469** (2014) 52. <https://doi.org/10.1016/j.apcata.2013.09.054>
- 2 M. Peymani, S. M. Alavi, and M. Rezaei: *Appl. Catal. A* **529** (2017) 1. <https://doi.org/10.1016/j.apcata.2016.10.012>
- 3 C. Cheephat, P. Daorattanachai, S. Devahastin, and N. Laosiripojana: *Appl. Catal. A* **563** (2018) 1. <https://doi.org/10.1016/j.apcata.2018.06.032>
- 4 M. Peymani, S. M. Alavi, and M. Rezaei: *Int. J. Hydrogen Energy* **41** (2016) 6316. <https://doi.org/10.1016/j.ijhydene.2016.03.033>
- 5 A. G. Dedov, A. S. Loktev, D. A. Komissarenko, K. V. Parkhomenko, A. C. Roger, O. A. Shlyakhtin, G. N. Mazo, and I. I. Moiseev: *Fuel Process. Technol.* **148** (2016) 128. <https://doi.org/10.1016/j.fuproc.2016.02.018>
- 6 D. Kaddeche, A. Djaidja, and A. Barama: *Int. J. Hydrogen Energy* **42** (2017) 15002. <https://doi.org/10.1016/j.ijhydene.2017.04.281>
- 7 J. H. Jun, T. H. Lim, S. W. Nam, S. A. Hong, and K. J. Yoon: *Appl. Catal. A* **312** (2006) 27. <https://doi.org/10.1016/j.apcata.2006.06.020>
- 8 A.S. Brayko, A. B. Shigarov, V. A. Kirillov, V. V. Kireenkov, N. A. Kuzin, V. A. Sobyenin, P. V. Snytnikov, and V. V. Kharton: *Mater Lett.* **236** (2019) 264. <https://doi.org/10.1016/j.matlet.2018.09.175>
- 9 M. Peymani, S. M. Alavi, and M. Rezaei: *Int. J. Hydrogen Energy* **41** (2016) 19057. <https://doi.org/10.1016/j.ijhydene.2016.07.072>
- 10 S. Chianese, S. Fail, M. Binder, R. Rauch, H. Hofbauer, A. Molino, A. Blasi, and D. Musmarra: *Catal. Today* **277** (2016) 182. <https://doi.org/10.1016/j.cattod.2016.04.005>
- 11 N. García-Moncada, M. González-Castaño, S. Ivanova, M. Á. Centeno, F. Romero-Sarria, and J. A. Odriozola: *Appl. Catal. B* **238** (2018) 1. <https://doi.org/10.1016/j.apcatb.2018.06.068>
- 12 S. M. Hashemnejad and M. Parvari: *Chin. J. Catal.* **32** (2011) 273. [https://doi.org/10.1016/S1872-2067\(10\)60175-1](https://doi.org/10.1016/S1872-2067(10)60175-1)
- 13 M. Khajenoori, M. Rezaei, and B. Nematollahi: *J. Ind. Eng. Chem.* **19** (2013) 981. <https://doi.org/10.1016/j.jiec.2012.11.020>
- 14 H. E. Figen and S. Z. Baykara: *Int. J. Hydrogen Energy* **40** (2015) 7439. <https://doi.org/10.1016/j.ijhydene.2015.02.109>
- 15 P. Corbo and F. Migliardini: *Int. J. Hydrogen Energy* **32** (2006) 55. <https://doi.org/10.1016/j.ijhydene.2006.06.032>
- 16 M. S. Venkatesh and G. S. V. Raghavan: *Biosyst. Eng.* **88** (2004) 1. <https://doi.org/10.1016/j.biosystemseng.2004.01.007>
- 17 W. Klinbun and P. Rattanadecho: *Appl. Math. Modell.* **36** (2012) 813. <https://doi.org/10.1016/j.apm.2011.07.003>
- 18 H. R. Prakruthi, B. S. Jai Prakash, and Y. S. Bhat: *J. Mol. Catal. A* **408** (2015) 214. <https://doi.org/10.1016/j.molcata.2015.07.036>
- 19 H. Demir: *Appl. Therm. Eng.* **50** (2013) 134. <https://doi.org/10.1016/j.applthermaleng.2012.06.022>
- 20 F. Motasemi, A. A. Salema, and M. T. Afzal: *Fuel Process. Technol.* **131** (2015) 370. <https://doi.org/10.1016/j.fuproc.2014.12.006>
- 21 W. Cai, C. Fu, W. Hu, G. Chen, and X. Deng: *J. Alloys Compd.* **554** (2013) 64. <https://doi.org/10.1016/j.jallcom.2012.11.154>
- 22 C. J. G. Jou, C. L. Lee, C. R. Wu, S. C. Hsieh, and P. K. A. Hong: *Environ. Chem. Lett.* **9** (2011) 355. <https://doi.org/10.1007/s10311-010-0286-y>
- 23 C. L. Lee, C. Lin, and C. J. G. Jou: *J. Air Waste Manage. Assoc.* **6** (2012) 1443. <https://doi.org/10.1080/10962247.2012.719579>
- 24 C. L. Lee and C. J. G. Jou: *Environ. Pollut.* **1** (2012) 159. <https://doi.org/10.5539/ep.v1n2p159>
- 25 I. Suelves, M. J. Lázaro, R. Moliner, B. M. Corbella, and J. M. Palacios: *Int. J. Hydrogen Energy* **30** (2005) 1555. <https://doi.org/10.1016/j.ijhydene.2004.10.006>